Size-selective resonant Raman scattering in CdS doped glasses

L. Saviot, B. Champagnon, and E. Duval
Laboratoire de Physico-Chimie des Matériaux Luminescents, UMR 5620 CNRS, Université Lyon I, 69622 Villeurbanne Cedex, France

A. I. Ekimov
A. F. Ioffe Physico-Technical Institute, 194021 St. Petersburg, Russian Federation
(Received 23 July 1997)

The size and excitation dependence of resonant low-frequency Raman scattering in CdS nanocrystals (radii less than 10 nm) embedded in a glassy matrix have been investigated. We report a size-selective excitation for excitations inside the absorption features. The Raman spectra exhibit a different behavior when the excitation is below the absorption band. This behavior is shown to depend on the fabrication process of the samples and is assigned to a resonance on surface defects.
[S0163-1829(98)01501-X]

I. INTRODUCTION

The original properties of semiconductor nanoparticles compared to the bulk materials have been at the origin of the large interest in these materials in the last decades.[1] These properties are related to the confinement in the semiconductor nanocrystals (radii less than 10 nm) of the (quasi) particles (electrons, holes, excitons, phonons, etc.).

Among these materials, the semiconductor doped glasses, some of which are commercially available as colored glasses, have been widely investigated for their optical properties. The electron-phonon coupling in these materials is of prime importance because its strength increases with decreasing nanocrystal size.[2] Confined acoustic and optical phonons were observed both in spectral hole burning[3] and photoluminescence experiments.[4] These results show the importance of a complete study of the confined vibration modes of the nanocrystals. Raman scattering is a suitable tool to access the vibration energies and also the electron-phonon coupling.[5,6] Previous results on CdSe-doped glasses have already shown that the effect of size is clearly seen on the acoustic modes.[7]

The present work is a study in CdS nanoparticles of the low-frequency inelastic scattering (LOFIS) that result from the Raman scattering of confined acoustic vibrations of the lattice.[8] It was conducted to take full advantage not only of the size variation, but also of the excitation energy variation. Original experimental results coming from the excitation dependence of the spectra were obtained. Their interpretation requires a new look at previously reported Raman results in CdS (Refs. 9 and 10) and CdS_xSe_{1-x} (Refs. 11–15) doped glasses.

II. SAMPLES AND EXPERIMENTAL PROCEDURE

The main part of this work was done on CdS nanoparticles obtained in a borosilicate glass matrix during a thermal annealing process based on diffusion controlled phase decomposition.[16] All experimental results reported here were obtained at room temperature. The average radius of the nanoparticles were measured by small-angle x-ray scattering (SAXS) and their absorption spectra were used to perform resonant Raman scattering. Two sets of samples with different particle concentrations were investigated. Unless stated differently, we will refer in the following to the most concentrated samples. Other samples prepared via a sol-gel route[17] were also investigated.

A five gratings DILOR Z40 monochromator was used to measure all the Raman spectra. Its high rejection rate makes it possible to measure low-frequency Raman spectra close to the Rayleigh line. Both backscattering and 90° geometries were used and no difference between them was observed. Different visible lines of Ar^+ and Kr^+ lasers were used for excitation.

Concerning the required excitation power, very different situations can be obtained because of the fast variation of the optical density of the samples. Special care was taken not to heat locally. This is achieved with low power in the spectral region of high absorption of the sample and higher power when the excitation is outside the absorption features to obtain a better signal-to-noise ratio. The Stokes-anti-Stokes ratio, a conventional way to check the temperature, could not be used because of the resonant conditions. Nevertheless, we could have some estimation of the local heating of the sample by checking the linearity of the signal with the excitation power. In the spectral range of fast variation of the optical density of our sample, some strong nonlinearity was observed, coming from the red shift of the absorption spectra with increasing temperature. A small local heating of the sample results in a significant increase in the optical density at the excitation wavelength and thus to more heating. In this case, very low excitation power was used. This does not occur in the spectral region where the optical density varies slowly.

III. RESULTS

Results obtained under the previously described conditions are presented in Figs. 1–7. Both the Stokes (creation of a vibration, positive Raman Shift) and anti-Stokes (annihilation of a vibration, negative Raman Shift) scattering are plotted in the LOFIS spectra.

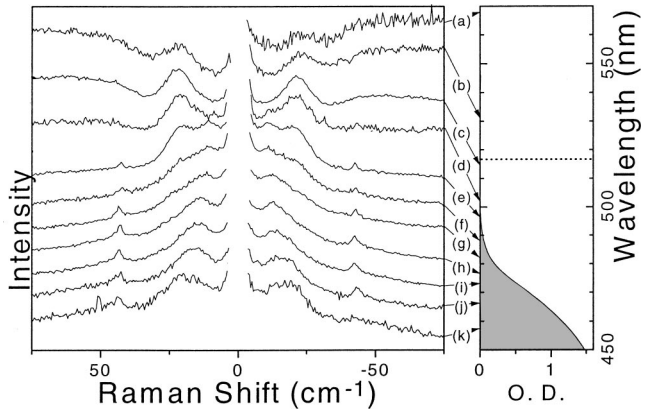

FIG. 1. Excitation dependence of the LOFIS spectra in a CdS-doped glass with an average radius $a=33$ Å. The right plot is the absorption spectrum of this sample and the arrows indicate the position of the excitation. The excitations used are 568.2, 530.9, 514.5, 501.7, 496.5, 488.0, 482.5, 476.5, 472.7, 465.8, and 457.9 nm from (a) to (k), respectively. The dotted line on the right plot indicates the position of the bulk wurtzite CdS gap.

Figures 1 and 2 are the excitation dependence of the LOFIS spectra of samples with average radius of the particles $a=33$ Å and $a=19$ Å, respectively. They show a strong dependence on the excitation energy. The experimental curves were normalized on their maximum to have comparable intensities. Absorption spectra are plotted to show the resonant condition of the different spectra. When the excitation is very far from the absorption structure, the observed scattering is the ''boson peak'' typical of the glass matrix[18] with a broad maximum around 50 cm^{-1}. This is the case for $a=19$ Å, $\lambda_{exc}=514$ nm (Fig. 2, curve a) and for $a=33$ Å, $\lambda_{exc}=647$ nm (same spectra as before, not shown in Fig. 1) and larger wavelengths. In these cases, no scattering around 303 cm^{-1} (position of the LO line of CdS) is observed. In all other cases plotted in these two figures, the 303 cm^{-1} LO line of CdS is seen. Two excitation domains (with some overlapping) can be distinguished: (a) inside

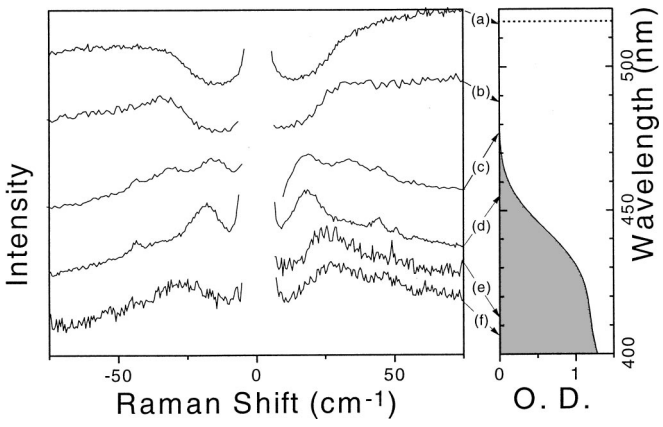

FIG. 2. Excitation dependence of the LOFIS spectra in a CdS-doped glass with an average radius $a=19$ Å. The right plot is the absorption spectrum of this sample and the arrows indicate the position of the excitation. The excitations used are 514.5, 488.0, 476.5, 457.9, 413.1, and 406.7 nm from (a) to (f), respectively. The dotted line on the right plot indicates the position of the bulk wurtzite CdS gap.

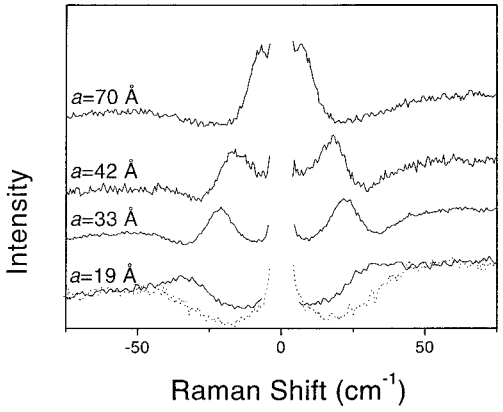

FIG. 3. Size dependence of the LOFIS scattering from CdS-doped glasses for excitation below the absorption bands. The spectra were obtained in the parallel configuration, except for the dotted curve that was obtained in the crossed configuration. The average radius a of the particles in the samples are indicated.

the absorption band (Fig. 1, curves $e-k$ and Fig. 2, curves $c-f$) where the position of the LOFIS line depends on the excitation; (b) below the absorption band (Fig. 1, curves $a-e$ and Fig. 2, curves b and c) where the shape and position of the Raman line are excitation-independent.

Figure 3 represents the size dependence of the LOFIS signal for excitation below the absorption features for different samples corresponding to average particle radius between 19 and 70 Å. A clear shift to lower energy as the average size of the particles increases is seen (see Fig. 5).

The polarized Raman spectra differ according to the excitation wavelength. Figure 4 compares for sample $a=33$ Å both kinds of excitation. Outside the absorption band ($\lambda_{exc}=514.5$ nm) LOFIS bands are strongly polarized. Only the boson peak of the glass is observed in the crossed configuration spectrum [Fig. 4a]. Inside the absorption band ($\lambda_{exc}=465.8$ nm) LOFIS bands are observed both in parallel and crossed polarization [Fig. 4b]: this corresponds to a strong depolarization of the light.

Figure 4 shows the LOFIS spectra in the parallel (electric field of incident and scattered light parallel) and crossed

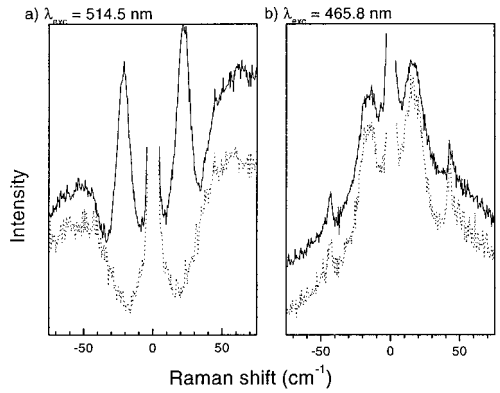

FIG. 4. Parallel (continuous curves) and crossed (dotted curves) configuration spectra of a CdS-doped glass with average particle radius $a=33$ Å. The excitation wavelengths λ_{exc} are given in the figure. The broad contribution around 50 cm^{-1} in both spectra with $\lambda_{exc}=514.5$ nm is the boson peak of the glass matrix. The relative intensities of both polarization configurations are not respected.

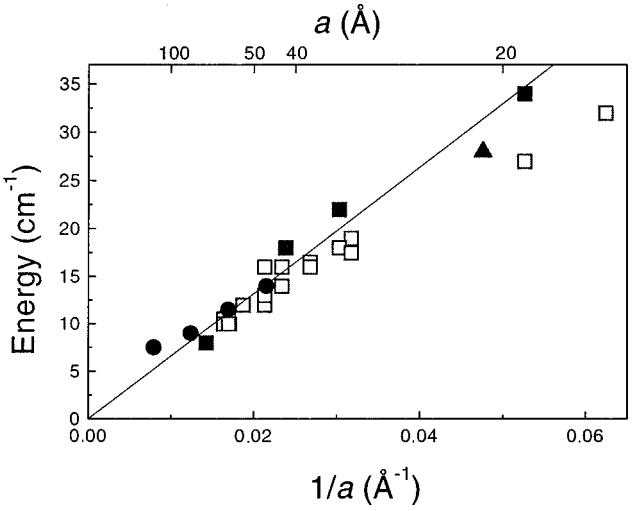

FIG. 5. Position of the low-frequency Raman lines as a function of the inverse radius. The full symbols correspond to excitations below the absorption and are plotted as a function of the average radii in the sample. The empty symbols correspond to the size-selective excitation of the particles and are plotted as a function of the excited size. Full circles and triangle are taken from the works of Tanaka and co-workers (Ref. 9) and Othmani (Ref. 10), respectively. The line is the best fit to our data as discussed in the text.

(electric field of incident and scattered light perpendicular) configurations for both kinds of excitation discussed before. The polarization behavior depends strongly on the excitation: below the absorption no depolarization is observed whereas a depolarized line is observed under resonant absorption conditions. This is the same whatever the sample and whatever the excitations in the two already described domains.

Figure 5 represents the position of the LOFIS line as a function of the inverse relevant radius as will be discussed later in the text.

Figure 6 shows the Raman cross section of the LOFIS and LO lines, to be compared with the absorption curve. To obtain this data, the absorption of the laser, the reabsorption of the Raman signal and the spectral response of the setup were taken into account. To do this, only the retro-Raman configuration was used to achieve a quantitative correction of both phenomena. With this geometry, it is not necessary to know the spatial shape of the laser beam. When changing the excitation wavelength, special care was taken not to disturb the alignment. Because this task is especially difficult, we believe our results are reliable to within 20%. This is enough to identify the position of the resonant transitions. Although the Raman cross section is much stronger when exciting into the absorption features than when exciting outside (Fig. 6), due to the absorption of the laser, the reabsorption of the signal and the heating effects described before, it is easier to obtain good spectra in the small absorption range where it is possible to use higher excitation power.

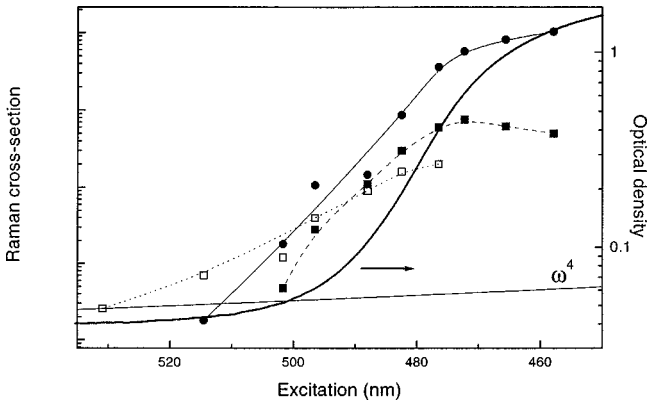

FIG. 6. Raman intensity for CdS nanoparticles (average radius 33 Å) as a function of the laser wavelength of the LO (full circles), depolarized LOFIS (full squares), and polarized LOFIS (empty squares) lines after correction of absorption. The thick line is the variation of the optical density of the sample. The ω^4 dependence expected for nonresonant scattering is also plotted.

Figure 7 shows the full Raman spectra obtained with excitation out of absorption, for two samples having approximately the same particle size but different fabrication process. One sample was obtained via a sol-gel route.[17] The intensity of the LOFIS line (compared to the LO line) depends strongly on the set of samples.

We can summarize the above results to point out some common features of all the obtained spectra: (a) the LOFIS line position is excitation dependent when the excitation is varied inside the absorption band; (b) the depolarization of the LOFIS lines depends very strongly on the position of the excitation. For all the samples, the LOFIS line is 100% polarized for excitation below the absorption edge while it is depolarized when exciting above; (c) the LOFIS line(s) and the 303 cm^{-1} LO line are seen under the same conditions.

All the results presented before concern the highest doped samples. Another set of samples with lower concentration and with smaller thickness was available. The experimental results concerning these samples are similar to those described before, except for excitations outside the absorption band where no Raman signal from the particles could be measured. This is just a manifestation of the important decrease in the efficiency of scattering when the excitation moves away from the absorption.

IV. DISCUSSION

In order to discuss the LOFIS lines, let's recall the well-known relation giving their position:[7]

$$\omega = S_{l,n}\,\frac{v}{2ac}, \tag{1}$$

where ω is the position in cm^{-1}, v is the longitudinal or transverse sound velocity expressed in the same unit as the light velocity c, and a is the radius of the particle expressed in cm. $S_{l,n}$ is a proportionality coefficient depending on the vibration mode angular momentum l and the harmonic number n, the chemical composition and shape of the particle, and the matrix.[7]

A. Excitation inside absorption: Size selection

A strong dependence of the LOFIS line position when changing the excitation wavelength is observed. For the sample of radius $a = 33$ Å, the position changes from 19 to 11 cm^{-1}. The LOFIS line position being inversely proportional to the radius of the particle [Eq. (1)] this means that

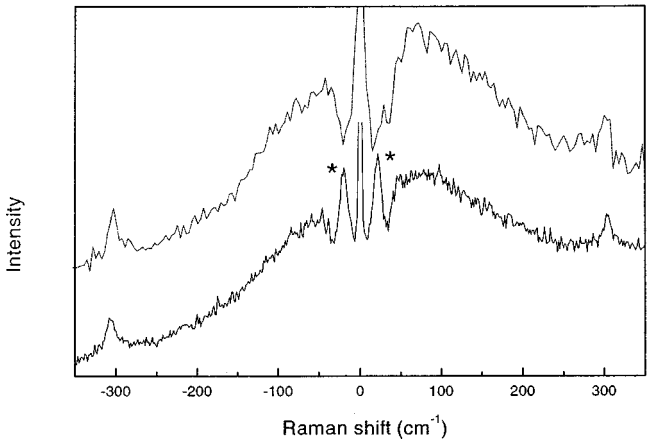

FIG. 7. Comparison of Raman spectra (excitation wavelength 514.5 nm) for two samples with different elaboration processes and matrices but close radii (bottom: $a=33$ Å, borosilicate glass and top: $a=37$ Å, sol-gel silica glass). The broad band around 50 cm^{-1} is the boson peak of the glass. The LO lines around ± 303 cm^{-1} are seen in both samples. The LOFIS lines ($*$), close to the Rayleigh line, are not seen in the sol-gel sample.

the more the excitation is shifted to the red, the larger the size of the scattering particles. This corresponds to a size-selective excitation that can exist when the homogeneous width of the electronic transition is smaller than the inhomogeneous one. Similar effects have been reported in luminescence experiment in CdSe nanoparticles.[19] To check the hypothesis of size-selective excitation, we plotted the position of this line as a function of the inverse excited radius with empty squares in Fig. 5. The excited radii were evaluated from the absorption spectra: we first derived the position of the first maximum of absorption by taking the second derivative of the spectra for different samples having different average size of nanoparticle. Then we plotted this position as a function of the average radius (obtained by SAXS) of the nanoparticles in our samples. By interpolating the resulting curve, we could make the conversion from wavelength to excited radius. The resulting points in Fig. 5 line up as expected from Eq. (1). This confirms that this depolarized LOFIS peak comes from the scattering by the resonantly excited nanoparticles only, and not from the full size distribution of nanoparticles.

Despite the number of works on this material, to the authors' knowledge, it is the first report of this behavior. Such phenomena may also exist in the LO Raman spectra, but the small dispersion of the LO phonon branch makes it difficult to observe it.

B. Excitation below absorption

The position of the polarized LOFIS peak is sample-dependent (see Fig. 3) but excitation-independent (see Figs. 1 and 2). Therefore we ascribe it to the scattering from all nanoparticles in the samples. To check it, we plotted with full squares in Fig. 5 the position of this line as a function of the inverse average radius of the nanoparticles in each sample. Once again, the points line up, validating our hypothesis.

Points coming from both the polarized and depolarized peaks line up on a same line. The slope of this line is proportional to $S_{l,n}$ [Eq. (1)] and therefore characterizes the vibration mode. Different slopes therefore correspond to different vibration modes, excepted for some accidental degeneracy. The best fit to this line gives $S=0.98$. The calculated values of $S_{l,n}$ (Table I) don't show such degeneracy around this value. (We estimate the experimental position of the LOFIS peaks to be reliable within ± 1 cm^{-1} that means that the experimental slope accuracy is around $\pm 10\%$). According to Duval,[20] only $l=0$ and $l=2$ modes are Raman active, and only the $l=0$ modes give polarized scattering. Because for excitation below absorption we can observe polarized lines, we attribute these LOFIS modes to ($l=0$, $n=0$) modes with the free-surface boundary condition corresponding to $S_{0.0}=0.91$.

TABLE I. Values of $S_{l,n}$ to be used with the longitudinal sound velocity as v in Eq. (1). The sound velocities used for this calculation are $v_l=4300$ ms^{-1} and $v_t=1860$ ms^{-1} (Ref. 24).

$S_{l,n}$	Free surface			Fixed surface		
l	0	1	2	0	1	2
$n=0$	0.91	0.51	0.37	1.43	0.64	0.89
$n=1$	1.96	1.01	0.72	2.46	0.88	1.16
$n=2$	2.97	1.36	1.20	3.47	1.29	1.49

Different hypotheses can be made to explain the depolarized lines observed for absorption resonant excitation: (a) to satisfy the selection rules predicted by Duval[20] for perfectly spherical nanoparticles and nonresonant excitations, the observed scattering is due to the ($l=2$, $n=1$ and 2) modes ($S_{2,1}=0.72$, $S_{2,2}=1.20$), these two modes having similar intensities that prevent us to resolve the two lines, or (b) the depolarized lines result from the scattering by ($l=0$, $n=0$) modes, the same as for the polarized lines, the different polarization behavior being due to the resonant nature of the process, or (c) the depolarized lines result from the scattering by ($l=1$, $n=1$) modes ($S_{l,l}=1.01$). Such modes are Raman inactive[20] but were found to become Raman active under resonant conditions in the case of optical vibrations.[21] In this case, the rough method used to determine the value of the radius of the excited CdS nanoparticles should be held responsible of the accidental coincidence of the points in Fig. 5.

C. Nature of the Raman line at 43 cm^{-1}

In the above discussion of the spectra, we disregarded a narrow line that appears in the LOFIS spectra (Figs. 1, 2, and 4) around 43 cm^{-1}. The position of this line is excitation- and sample-independent. It is therefore not a LOFIS line in the sense that it does not come from the confinement of acoustic vibrations.

Bulk CdS has the hexagonal wurtzite-type structure (noted W) in normal conditions. The main Raman peak comes from the 303 cm^{-1} optical mode.[22] A lot of other features are also reported due to the nine optical branches. One of them is of special interest in this work because of its spectral position: the 43 cm^{-1} optical mode. The observation of this line confirms the wurtzite structure of the nanoparticles because this mode does not exist in the blende structure at the center of the Brillouin zone.[23] This line is not

observed far from resonances and in low-concentrated samples because of its small Raman cross section.

D. Nature of the resonances

When exciting inside the absorption, as seen from Fig. 6, there is a strong increase in the Raman cross section. In this case, the resonant transitions are those coming from the carriers inside the CdS nanoparticles. When the excitation is below the absorption, the Raman cross section of the polarized LOFIS line increases much faster than the ω^4 law expected for nonresonant scattering (also plotted in Fig. 6). Therefore, there is still a resonance. No significant absorption is seen in the absorption spectra around these wavelengths. From Fig. 7, we can see that the ratio polarized LOFIS/LO depends on the elaboration process of the sample. We could check experimentally that the behavior for absorption resonant excitation is the same for both samples. So we believe that the transitions giving rise to this resonance process involve defects. Because the observed vibration mode ($l=0$, $n=0$) have a maximum deformation at the surface of the nanoparticles, the involved defects are probably located at the surface of the CdS nanoparticles. The relative intensity of the polarized LOFIS vs the LO peak is then a way to measure the number of surface defects in such kind of samples.

E. Comparison with previous works

The experimental results obtained by Tanaka and co-workers[9] and Othmani[10] fit very well with our ones, as seen in Fig. 5. The polarization behavior already described are also observed in these experiments. It should be noticed that the use of only one excitation energy to characterize the samples can be the source of wrong interpretations, due to the size-selective excitation. The attribution of all the LOFIS line to a single nanoparticle size is erroneous.[9] The good agreement between all these different experimental results is a proof that we are dealing with a general behavior of CdS nanoparticles in glasses because the preparation of the samples are different.

In CdS_xSe_{1-x}-doped glasses, both the polarized and the depolarized LOFIS lines are reported[11–14] and are correlated to the spectral position of the laser with respect to the absorption spectra of the sample in the same way as that for CdS.

F. Nature of the acoustic modes

In a previous paper about CdSe nanoparticles,[7] we could observe three different acoustic modes related to one single size. The present results only consist in one LOFIS line in each of the resonant conditions. Two lines can be observed in the overlap of these regions and therefore they correspond to two different sizes because one of the resonance is size selective. So the broadening model presented in[7] cannot give much information here. We would like to give some arguments to explain the observed differences between the two very similar materials. The Bohr exciton radius of CdSe is around 54 Å and the samples measured in Ref. 7 have radius below 40 Å. They all belong to the strong confinement regime. The Bohr exciton radius of CdS is around 29 Å that means that our bigger sample ($a=70$ Å) nearly belongs to the weak confinement regime while the other ones belong to the intermediate confinement one. Only the smaller size ($a=19$ Å) can be compared to CdSe. Because the excitation is size selective, only the smaller wavelength (406 and 413 nm) corresponds to excited sizes smaller than the Bohr exciton radius. For these two wavelengths, the signal to noise ratio is poor because of the low excitation power required not to heat the sample, the absorption and reabsorption phenomena and also the poor response of our monochromator. Anyway, Fig. 2, curve *f* shows two bands, one at 32 cm^{-1} and another broad one around 50 cm^{-1}. It means that CdS and CdSe nanoparticles have similar behavior when they are investigated under the same conditions. This also shows that resonant Raman scattering from acoustic confined vibrations is a good tool to access information about the nature of the resonant electronic transition.

V. CONCLUSION

In this work, we have demonstrated the interest of the LOFIS method in the study of CdS nanoparticles embedded in glasses. The changes in the spectra with the change of the excitation wavelength have been interpreted in term of resonances. The confined electron-hole transitions, which give rise to the increase of the «gap» with decreasing nanoparticle size, leads to size selection under resonant excitation. Another resonant situation is also reported which involves defects at the surface of the nanoparticles. These two resonances have to be taken into account when characterizing such nanoparticles and their defects. They also can be used to study the coupling between confined electron-hole pairs and confined acoustic vibrations.

ACKNOWLEDGMENTS

We would like to thank, M. Pauthe, A. Pradel, M. Ribes, and A. Ross, from Laboratoire de Physico-Chimie de la Matière Condensée UMR 5617 CNRS-Université Montpellier II for providing the sol-gel samples.

[1] L. Banyai and S. W. Koch, *Semiconductor quantum dots* (World Scientific, Singapore, 1993), and references therein.

[2] S. Schmitt-Rink, D. A. Miller, and D. S. Chemla, Phys. Rev. B **35**, 8113 (1987).

[3] S. Okamoto and Y. Masumoto, J. Lumin. **64**, 253 (1995).

[4] U. Woggon, F. Gindele, O. Wind, and C. Klingshirn, Phys. Rev. B **54**, 1503 (1996).

[5] M. C. Klein, F. Hache, D. Ricard, and C. Flytzanis, Phys. Rev. B **42**, 11 123 (1990).

[6] A. P. Alivisatos, T. D. Harris, P. J. Caroll, M. L. Steigerwald, and

L. E. Brus, J. Chem. Phys. **90**, 3463 (1989).
[7] L. Saviot, B. Champagnon, E. Duval, I. A. Kudriavtsev, and A. I. Ekimov, J. Non-Cryst. Solids **197**, 238 (1996).
[8] E. Duval, A. Boukenter, and B. Champagnon, Phys. Rev. Lett. **56**, 2052 (1986).
[9] A. Tanaka, S. Onari, and T. Arai, Phys. Rev. B **47**, 1237 (1993).
[10] A. Othmani, thesis Université Lyon I, 1994.
[11] B. Champagnon, B. Andrianasolo, and E. Duval, J. Chem. Phys. **94**, 5237 (1991).
[12] B. Champagnon, B. Andrianasolo, and E. Duval, Mater. Sci. Eng. B **9**, 417 (1991).
[13] K. E. Lipinska-Kalita, G. Mariotto, and E. Zanghellini, Philos. Mag. B **71**, 547 (1995).
[14] B. Champagnon, B. Andrianasolo, A. Ramos, M. Gandais, M. Allais, and J. P. Benoit, J. Appl. Phys. **73**, 2775 (1993).
[15] A. Roy and A. K. Sood, Solid State Commun. **97**, 97 (1996).
[16] A. I. Ekimov, Radiat. Eff. Defects Solids **134**, 11 (1995).
[17] J.-L. Marc, thesis, Université Montpellier II, 1994.
[18] A. P. Sokolov, A. Kisliuk, D. Quitmann, and E. Duval, Phys. Rev. B **48**, 7692 (1993).
[19] P. A. M. Rodrigues, G. Tamulaitis, P. Y. Yu, and S. H. Risbud, Solid State Commun. **94**, 583 (1995).
[20] E. Duval, Phys. Rev. B **46**, 5795 (1992).
[21] M. P. Chamberlain, C. Trallero-Giner, and M. Cardona, Phys. Rev. B **51**, 1680 (1995).
[22] B. Tell, T. C. Damen, and S. P. S. Porto, Phys. Rev. **144**, 771 (1966).
[23] M. A. Nusimovici and J. L. Birman, Phys. Rev. **156**, 925 (1967).
[24] D. Gerlich, J. Phys. Chem. Solids **28**, 2575 (1967).